Naval Research Laboratory
Stennis Space Center, MS 39529-5004

NRL/MR/7175--95-7573

Modeling Backscattering from a Rough Seafloor with Sediment Inhomogeneities

JORGE C. NOVARINI

Planning Systems Inc.
Slidell, LA 70458
Prepared for Acoustics Division

JERALD W. CARUTHERS

Ocean Acoustics Branch
Acoustics Division

DTIC
SELECTE
MAR 14 1995
B

DTIC QUALITY INSPECTED 4

February 27, 1995

19950310 038

Approved for public release; distribution is unlimited.

REPORT DOCUMENTATION PAGE

Form Approved
OBM No. 0704-0188

Public reporting burden for this collection of information is estimated to average 1 hour per response, including the time for reviewing instructions, searching existing data sources, gathering and maintaining the data needed, and completing and reviewing the collection of information. Send comments regarding this burden or any other aspect of this collection of information, including suggestions for reducing this burden, to Washington Headquarters Services, Directorate for information Operations and Reports, 1215 Jefferson Davis Highway, Suite 1204, Arlington, VA 22202-4302, and to the Office of Management and Budget, Paperwork Reduction Project (0704-0188), Washington, DC 20503.

1. AGENCY USE ONLY *(Leave blank)*	2. REPORT DATE	3. REPORT TYPE AND DATES COVERED
	February 27, 1995	Final

4. TITLE AND SUBTITLE

Modeling Backscattering from a Rough Seafloor with Sediment Inhomogeneities

5. FUNDING NUMBERS

Job Order No. 571525305
Program Element No. 062435N, 061153N
Project No.
Task No. RL3B, LR030243
Accession No. DN154087, DN152059

6. AUTHOR(S)

Jorge C. Novarini* and Jerald W. Caruthers

7. PERFORMING ORGANIZATION NAME(S) AND ADDRESS(ES)

Naval Research Laboratory
Acoustics Division
Stennis Space Center, MS 39529-5004

8. PERFORMING ORGANIZATION REPORT NUMBER

NRL/MR/7175--95-7573

9. SPONSORING/MONITORING AGENCY NAME(S) AND ADDRESS(ES)

Office of Naval Research
800 N. Quincy St.
Arlington, VA 22217

10. SPONSORING/MONITORING AGENCY REPORT NUMBER

11. SUPPLEMENTARY NOTES

*Planning Systems Inc., Slidell, LA 70458

12a. DISTRIBUTION/AVAILABILITY STATEMENT

Approved for public release; distribution unlimited.

12b. DISTRIBUTION CODE

13. ABSTRACT *(Maximum 200 words)*

Current models used to predict the backscattering strength of the ocean floor are either very involved, requiring geoacoustic parameters usually unavailable for the site in practical applications, or overly simplistic, relying mainly on empirical terms such as Lambert's law. In any case, solutions are very approximate and the problem is still far from being solved. In this work, a model is presented that avoids empirical functional forms, yet requires only a few physical parameters to describe the surficial sediments, often tabulated for typical sediments. The aim of the work is to develop a simple algorithm for operational prediction of bottom reverberation with only one free parameter, i.e., the volume scattering coefficient. The algorithm combines a two-scale surface scattering model [Caruthers and Novarini, IEEE J. Oceanic Engr., v 18, p 100–107, 1993 and Novarini and Caruthers, IEEE, J. Oceanic Engr. v 19, p 200–207, 1994], with scattered contributions originating from inhomogeneities within the sediments, taking into consideration the rough interface [Ivakin and Lysanov, Sov. Phys. Acoust. v 27, p 212–215, 1981]. No specific mechanism is assumed for scattering at the volume inhomogeneities; however, the inhomogeneities are assumed to be uniform and isotropic. The volume scattering coefficient, combined with the bottom attenuation and density and referenced to the surface, plays a role similar to the Lambert's constant in empirical models. The model is exercised on a variety of published datasets for low and moderately high frequency. In general, the model performs very well for both fast and slow sediments, showing a definite improvement over Lambert's law.

14. SUBJECT TERMS

MCM sonar system designs, shallow water acoustics,
ocean scattering, high frequency acoustics

15. NUMBER OF PAGES

24

16. PRICE CODE

17. SECURITY CLASSIFICATION OF REPORT	18. SECURITY CLASSIFICATION OF THIS PAGE	19. SECURITY CLASSIFICATION OF ABSTRACT	20. LIMITATION OF ABSTRACT
Unclassified	Unclassified	Unclassified	SAR

MODELING BACKSCATTERING FROM A ROUGH SEAFLOOR WITH SEDIMENT INHOMOGENEITIES

Jorge C. Novarini, Planning Systems, Inc., Slidell, LA 70458
Jerald W. Caruthers, Naval Research Laboratory,
Stennis Space Center, MS 39529

ABSTRACT

Current models used to predict the backscattering strength of the ocean floor are either very involved, requiring geoacoustic parameters usually unavailable for the site in practical applications, or overly simplistic, relying mainly on empirical terms such as Lambert's law. In any case, solutions are very approximate and the problem is still far from being solved. In this work, a model is presented that avoids empirical functional forms, yet requires only a few physical parameters to describe the surficial sediments, often tabulated for typical sediments. The aim of the work is to develop a simple algorithm for operational prediction of bottom reverberation with only one free parameter, i.e., the volume scattering coefficient. The algorithm combines a two-scale surface scattering model [Caruthers and Novarini, IEEE J. Oceanic Engr, v 18, p 100-107, 1993 and Novarini and Caruthers, IEEE, J. Oceanic Engr, v 19, p 200-207, 1994], with scattered contributions originating from inhomogeneities within the sediments, taking into consideration the rough interface [Ivakin and Lysanov, Sov.Phys. Acoust. v 27, p 212-215, 1981]. No specific mechanism is assumed for scattering at the volume inhomogeneities; however, the inhomogeneities are assumed to be uniform and isotropic. The volume scattering coefficient, combined with the bottom attenuation and density and referenced to the surface, plays a role similar to the Lambert's constant in empirical models. The model is exercised on a variety of published datasets for low and moderately high frequency. In general, the model performs very well for both fast and slow sediments, showing a definite improvement over Lambert's law.

I. INTRODUCTION

Scattering from the seafloor has been the subject of many papers in the last forty years. However, in spite of these many efforts, the problem is far from being solved. Acoustic bottom interaction is an extremely complicated physical phenomenon, since it involves scattering at a statistically rough penetrable surface overlaying an inhomogeneous viscoelastic medium. Each of these phenomena are individually complex and their combined effect is almost unmanageable. An additional complication is that some characteristics of the sediments are difficult to measure, and

Avail and/or
Dist Special
A-1

detailed bottom structure is known only over very limited geographical regions. Moreover acoustic experiments on bottom interaction are not, as a rule, accompanied by the geophysical information necessary to model adequately the data or interpret the results. As a consequence, models may quickly become complicated and justification weak.

In the past, bottom reverberation was considered to be produced mainly at the water-sediment interface, with possible contributions from subbottom rough interfaces. In the last few years evidence has accumulated which indicates that scattering at volume inhomogeneities within the sediment is a strong contributor, and this has stimulated an increased interest in the subject.[1-6] Although early attempts were made to evaluate the scattering strength produced within the sediment, these dealt with volume scattering from a medium bounded by a flat interface (Stockhausen[7] and Zhitkovskii[8]). In a clever and elegant paper, Crowther[1] considered both bottom roughness and volume scattering; but when dealing with the latter contribution a flat interface was implicitly assumed.

The pioneer work on the volume scattering contribution, including the effects of the rough boundary, can be credited to Ivakin and Lysanov.[9] Their volume scattering component was based on an isotropic distribution of scatters beneath a surface that was rough in the large scale. The contribution of volume scatters was averaged over the distribution of slopes. The averaging process was a little awkward and they did not include a separate surface roughness scattering mechanism. Following the approach of Ivakin and Lysanov, Jackson and his co-workers[2,3] developed a model that included separate surface scattering terms. They adopted Stockhausen's model for the volume contribution, and carried out the large-scale slope averaging process numerically. Recently, Lyon et al.[10] extended Jackson's work to include specific volume scattering mechanisms and scattering at the subbottom interface.

Most current efforts in the research community are concentrated on modeling bottom backscattering making use of an increasing number of geoacoustic parameters (e.g., sound speed gradient in the sediments, fluctuations in compressibility and in the density, stratification, attenuation). However, most of those parameters are usually unavailable and, as a matter of fact, no firm experimental evidence exists to support any specific scattering mechanism requiring such a detailed description.

The intricacies of this approach stand in stark contrast to the simplicity of Lambert's law, which is currently used for most sonar applications. Lambert's law requires a single empirical coefficient, which was established by Mackenzie,[11] based on a limited dataset taken in the early 1960's, to be -27 dB. Work is currently in progress to develop values for the Lambert constant on a regional basis (Geddes[12]). However, Lambert's law has shortcomings. It has a cosine-squared angular functional

form which sometimes fails to fit data, especially at lower grazing angles, and it is inappropriate for near-specular scatter (i.e., near-normal backscatter and forward scatter). To mediate against this latter problem, Lambert's law is sometimes combined with some near-specular scattering algorithm.[13,14] One of these algorithms, the rough facet model (RFM), uses a two-scale surface scattering model for predicting the specular lobe, and resorts to Lambert's law for directions away from specular.[14]

To replace the Lambert term, this present work combines the rough facet model with a volume scattering component based on the work of Ivakin and Lysanov,[9] and implements resonant (Bragg) scattering at the microroughness scale. The seafloor is assumed to be a fluid containing isotropic volume inhomogeneities witn no stratification. The model uses the volume scattering cross-section of the sediment as a free parameter which, combined with the sediment attenuation and density, plays a role analogous to the Lambert constant. The basic aim of this work is to provide a simple model for predicting the bottom backscattering strength which avoids empirical expressions (such as Lambert's law) while keeping the calculations and input requirements at a minimum. No attempt is made here to connect the resulting volume scattering strength with a specific volume scattering mechanism. It is shown that the overall performance is satisfactory, and constitutes a definite improvement over Lambert's law in fitting a variety of datasets.

II. DESCRIPTION OF THE SCATTERING MODEL

The backscattering coefficient of the seafloor, m_{bs}, is assumed to be made-up of three contributions:

$$m_{bs} = m_f + m_\mu + m_v \,, \qquad (1)$$

where m_f represents the scattering contribution from fine-scale components of the bottom roughness (geomorphology at a scale just below large-scale, deterministic bathymetry but larger than an acoustic wavelength) within the footprint of ensonification; m_μ is the contribution from the micro-scale roughness (microroughness), and m_v is the contribution from the inhomogeneities within the volume of the sediments, with due regard to the fact that it comes through the rough interface. Henceforth, this last contribution will be referred to as the "volume-induced bottom scattering coefficient". The large-scale roughness components, associated with long surface wavelengths present in bathymetric databases are handled deterministically and are excluded from this analysis (i.e., as a tilt in the footprint which is removed deterministically). The quantity $10\log(m_{bs})$ is the bottom backscattering strength in dB. The individual terms in Eq. (1) may also be expressed in dB. Generally, there is only a small angular range in which the terms must be added in their magnitude quantities.

The Rough Facet Model

The first term (m_f) is handled by the rough facet model.[14] This term represents the collective contribution from reflections at the fine-scale facets containing microroughness. That is, it is controlled by a facet reflection process which is partially coherent for individual facets but collectively incoherent when summed over the sonar footprint. Additional fundamental assumptions in approach are that the facet slopes have a gaussian distribution over the footprint and that the source and receiver are in the farfield of the footprint.[15] The term has the form

$$m_f = M(k,\sigma_\mu,\theta) \cdot F(\delta_f,\theta) , \qquad (2)$$

where $M(\cdot)$ is the coherent reflection coefficient due to the microroughness on a facet, and $F(\cdot)$ is the contribution of the fine-scale slopes of the facets. The additional parameters are: k is the acoustic wavenumber; σ_μ is the rms height of the microroughness; δ_f is the rms slope of the fine-scale facets; and θ is the local angle of incidence measured from normal. (We will later have use for the rms slope angle defined by $\alpha_f=\tan^{-1}\delta_f$.) The coherent reflection coefficient is given by

$$M = \exp(-g_\mu) , \qquad (3)$$

where g_μ is the roughness parameter of the microroughness, i.e.,

$$g_\mu = 4\,\sigma_\mu^{\,2}\,k^2\cos^2\theta . \qquad (4)$$

The function $F(\cdot)$ is the high-frequency limit of the Helmholtz/Kirchhoff theory.[15] For the case of monostatic backscattering this reduces to

$$F = \frac{R_o^{\,2}}{8\pi\delta_f^{\,2}\cos^4\theta} \exp\left[-\frac{\tan^2\theta}{2\delta_f^{\,2}}\right] , \qquad (5)$$

where R_o is the pressure-reflection coefficient of the sediment, assuming it to be a fluid. As in any two-scale roughness theory, the choice of the partition wavenumber between the fine-scale roughness and the microroughness is crucial to the results.

Power spectra used to describe seafloor roughness are most often of the isotropic power-law form,

$$W(K) = a^2\,K^{-2b} , \qquad (6)$$

where K is the spatial frequency of the surface roughness (i.e., the reciprocal wavelength in cycles/meter). (Note our use of the spatial frequency K for surface specifications and the wavenumber k for acoustics applications.)

It should be noted that, in the rough facet model, the two surface parameters (the rms height of the micro-scale surface and the rms slope of the fine-scale surface) are bandlimited quantities. The variance of the microroughness for a 2-D isotropic surface is given by

$$\sigma_\mu^2 = 2\pi \int_{K_c}^{K_h} W(K)\, K\, dK . \qquad (7)$$

The variance of the slopes of the fine-scale surface by

$$\delta_f^2 = 2\pi \int_{K_l}^{K_c} W(K)\, K^3\, dK . \qquad (8)$$

In Eqs. (7) and (8), K_l and K_h indicate the low and high spatial frequencies present on the surface, respectively. These spatial frequencies are determined by the size of the footprint and the grid spacing, respectively. K_c denotes the partition (cut-off) spatial frequency. For analytical work K_h can approach infinity; but a K_l approaching zero would give rise to problems with the power-law spectrum, and is not physical because the footprint of a sonar is always limited in size.

A recent numerical study[16] has shown that the appropriate partition for the rough facet model is that which makes g_μ equal to unity. Under that condition, RFM models the specular lobe with high accuracy.

The reflection coefficient is given by

$$R_o = (u-1)/(u+1) , \qquad (9)$$

where

$$u = m \cos\theta \,/\, (n^2 - \sin^2\theta)^{1/2} . \qquad (10)$$

Since the sediment is considered a lossy medium in this work, the index of refraction n is complex, i.e.,

$$n = c/c_1 = n_0(1+i\phi), \quad \text{and} \quad m = \rho_1 / \rho ,$$

where c is velocity and ρ is density (parameters subscripted with "1" here and throughout are for the sediments). The parameter ϕ is the so-called "loss tangent" given by

$$\phi = \kappa_p \log_{10}(c_1) / 40\pi ,$$

where κ_p is the attenuation factor for compressional waves, defined as the attenuation coefficient in the sediment (dB/m) divided by frequency.[17] It has the units dB/(m-kHz) and frequency expressed in kHz.

Microroughness Scattering

In Eq. (2), the microroughness is only present as a loss mechanism in the specular direction (through the factor M). However, the microroughness re-scatters energy in all directions, including the receiver direction, and its contribution to the total scattering coefficient must be accounted for. Since, in the micro-scale, we are dealing with an acoustically smooth surface ($k\sigma_\mu < 1$), the contribution can be evaluated through perturbation theory, leading to resonant (Bragg) scattering. For this work we have adopted the expression given by Brekhovskikh and Lysanov[15] for Bragg scattering, modified for our definition of variance (Eq. (7)). It is less desirable to assume the validity of a plane-wave reflection coefficient for microroughness than for fine-scale roughness in the case of penetrable surfaces; nevertheless, we make this assumption to avoid major complexity that will later accompany reflection in bistatic scattering. Here we apply it to the monostatic case and isotropic penetrable surfaces. It allows Bragg scattering due to the microroughness that can be written as

$$m_\mu = R_o^2 \, k^2 \cos^2\theta \, W[2k\sin\theta] / \pi^2 , \qquad (11)$$

where the power density spectrum is evaluated at the resonant wavenumber. The validity of Eq. (11), however, is limited to angles that are greater than what might be called the "partition angle", which may be defined as the angle subtended by a facet. There are several reasons for this limit: (1) scattering would become infinite if the angle went to zero (i.e., the resonant wavenumber would tend to zero and the resonant wavelength and spectral density to infinity); and (2) the height difference for widely separated points on the surface violates the small perturbation assumption. Since the facet size was defined by $g_\mu = 1$, it is a reasonable limit for the validity of perturbation theory.

Figure 1 shows the contributions of m_f and m_μ to the scattering strength. Note that at wide angles m_μ exceeds m_f. It also exceeds m_f very near normal incidence, but this part we disregard based on the above considerations. We adopt the following

scheme for adding m_f and m_μ: m_μ will usually dip below m_f for some part of the angular range; where that difference (in dB) is the greatest (at θ_p) we start adding m_μ to m_f because the abrupt change has the least impact. For grazing angles smaller than this, the Bragg contribution becomes increasingly important, and is added to the rough facet model. The result is that, of the two terms, either m_f or m_μ dominates over most of the range with only a small region of transition. For very smooth surfaces, where there isn't sufficient microroughness or rms slope within the footprint, Bragg may dominate the rough facet model in all but the specular direction. We will see in the next section that at wider angles the volume scattering term will dominate, and in some cases it will take over before Bragg becomes significant.

The Volume Scattering Model

To estimate the contribution of m_v coming from the interior of the sediment through the rough interface we have adopted the Ivakin and Lysanov[9] formalism, which accounts for the volume contributions taking into account the rough boundary. In their work they assumed a uniform distribution of scatterers within the volume of the sediment. Since, to the authors knowledge, there is no conclusive evidence in the literature that supports any specific type of distribution for the random inhomogeneities, we have adopted the uniform distribution of isotropic scatterers, which is the simplest possible selection (the horizontal stratification of the sediment layers do not constitute the random scatters modeled in this work). In the present model, the scattering cross-section per unit volume (or volume scattering coefficient, m_o) is the only free parameter. Unfortunately, most of available datasets that can be used for testing the model do not provide the minimum necessary geoacoustical information to apply the model without requiring further "guesstimates". Hence, in all the cases examined in this work, other parameters beside m_o need to be estimated.

In the special case of monostatic backscattering and isotropic, weak, volume scattering the Ivakin/Lysanov model yields the following expression for the volume contribution to the bottom backscattering coefficient

$$m_v = \frac{m_o}{2\beta m^2} \left\langle \frac{T^4(\theta')[n^2-\sin^2\theta']^{1/2}}{n\cos\alpha} \right\rangle , \qquad (12)$$

where $\beta = 2k_1\phi$, $\theta' = \theta-\alpha$, and α is the local slope angle of the interface. The angle brackets represent a fine-scale slope average over the footprint. $T(\theta)$ is the local amplitude transmission coefficient given by

$$T(\theta) = 2\, m \cos\theta \,/\, [m\cos\theta + (n^2 - \sin^2\theta)^{1/2}] .$$

Since we want to keep the algorithm as simple as possible, averaging is accomplished simply by replacing the incidence angle by the incidence angle minus the rms slope (i.e., $<\theta'> = \theta - \alpha_f$). This is a reasonable approximation, since making the effective incidence angle larger will emphasize scattering at high grazing angles, i.e., more energy will enter the bottom on the upslope side than on the downslope side. Also, this can account heuristically for shadowing. To further simplify the modeling process, we use the bandlimited α_f value evaluated at $\theta=0$ (i.e., α_{fo}). Therefore, the estimated volume contribution is given by

$$m_v = \frac{m_o}{2\beta m^2} \left\langle \frac{T^4(\theta-\alpha_{fo})[n^2-\sin^2(\theta-\alpha_{fo})]^{1/2}}{n\cos\alpha_{fo}} \right\rangle . \qquad (13)$$

Finally, we rearrange Eq. (13) to produce the form

$$m_v = \mu_v \cdot V(\theta) , \qquad (14)$$

where

$$V(\theta) = \frac{\cos^4\theta\,[1-\sin^2\theta/n^2]^{1/2}\,(m+\sqrt{n^2})^4}{[m\cos\theta + (n^2 - \sin^2\theta)]^4} \qquad (15)$$

and

$$\mu_v = \frac{m_o\, 8m^2}{\beta\cos\delta_{fo}\,[m + \sqrt{n^2}\,]^4} \qquad (16)$$

The functional form $V(\theta)$ goes to unity as θ goes to zero (normal incidence). The constant μ_v is a surface scattering constant attributed to volume scattering; that is, it is a constant times an angular functional form referenced to the surface. In addition to showing the form of the first two terms in Eq. (1), and their combined effects, Fig. 1 also shows the relative contribution of the volume term m_v.

Much can be said of the functional form of $V(\theta)$, but here we limit our comments to pointing out that it can vary between $\cos\theta$ (Lommel/Zeeliger law[18]) at normal incidence through $\cos^2\theta$ (Lambert's law) at moderate grazing angles, to higher powers of cosine for near grazing. Many researchers have fitted backscattering data at moderate grazing with Lambert's law. In that case μ_L becomes an empirical fit to the theoretically derived μ_v. (Note, however, that μ_L is not numerically equal μ_v because $V(\theta)$ approaches normal incidence differently from Lambert's law.) In future work, μ_v

(and therefore the free parameter m_0) will be related to the type of sediment, in a manner similar to that which is sometimes done for the Lambert constant.

Since n is complex, the calculations of $R(\theta)$ and $T(\theta)$ are performed using the FORTRAN complex intrinsic functions in the computer implementation. Allowing for complex n constitutes another difference from the original Ivakin/Lysanov model. This is, however, consistent with later work by the same authors in connection with scattering from a flat bottom.[19] Complex n allows for attenuation in the bottom, which becomes a key factor near critical angle for a fast bottom.

III. RESULTS

The model will now be applied to a variety of available datasets. The idea is to examine the prospects for this simple functional form to yield reasonable results when fitting a wide range of experimental data. Table I list the datasets chosen for this study, the physiographical region, the surficial sediment (as listed in the original reference), and the code assigned to each dataset. Most of the data were extracted from the database developed by Li Zhang.[20] To provide a further distinction among the datasets, the code name assigned to each dataset has been modified from the designation in Zhang's database.

Table I: Datasets, locations, and codes.

DATASET	REGION	SEDIMENT*	CODE
Buckley and Urick[24]	Cont. Rise (Area II)	silt?	byuk68_A2
Buckley and Urick[24]	Cont. Rise (Area III)	------	byuk68_A3
Hines and Barry[4]	Abyss. Plain (Site A)	silt	hnby92_SA
Hines and Barry[4]	Abyss. Plain (Site C)	silt/sand	hnby92_SC
Jin et al.[21]	China Sea	clay	jnel89
Maradino et al.[26]	Abyss. Plain (Stn 1)	sand/silt	mogy85
Schmidt[22]	Norweign Sea (Stn 3)	------	scdt69_stn3
Schmidt[22]	Cont. Slope (Stn 5)	------	scdt69_stn5
Volovov & Zhitkovskiy[23]	N. Atlant (Stn 1)	------	vvzy74
Zotov and Fokin[25]	Clipperton Fault (Stn 2)	------	zvfn85

*Surficial sediment, as listed in the original reference

Table II: Geoacoustic and experimental parameters.

DATASET	f(kHz)	C_0	C_1	r_1	κ_p	a(x10^{+3})	b	δ_f(deg)	σ_μ(m)	Θ_p(deg)
byuk68_A2	2.8	1545	1585	1.6	0.15	1.2	1.62	0.2	0.04	0
byuk68_A3	2.8	1530	1510	1.7	0.10	1.2	1.62	0.2	0.04	0
hnby92_SA	0.9	1545	1680	1.6	0.04	1.2	1.62	0.1	0.13	0
hnby92_SA	1.2	1545	1680	1.6	0.04	1.2	1.62	0.2	0.04	0
hnby92_SA	2.3	1545	1680	1.6	0.04	1.2	1.62	0.2	0.05	0
hnby92_SC	2.3	1545	1550	1.6	0.15	1.2	1.62	0.2	0.05	0
jnel89	2.0	1530	1510	1.7	0.10	2.0	1.95	2.5	0.06	5
mogy85	0.365	1545	1650	2.0	0.09	1.2	1.95	0.7	0.33	0
scdt69_Stn3	3.2	1530	1528	2.0	0.10	2.0	1.95	2.7	0.04	5
scdt69_Stn5	3.2	1530	1528	2.0	0.10	2.0	1.95	2.7	0.04	5
vvzy74	5.0	1530	1510	1.7	0.10	2.0	1.62	0.7	0.02	0
zvfn85	4.0	1545	1784	2.0	0.70	2.0	1.62	0.9	0.03	0

Table II lists the parameters used for fitting the data (c_0, c_1, ρ_1, K_p, a, and b), and the related surface parameters α_{fo}, $\sigma_{\mu o}$, and θ_p. No precise geoacoustic data are available for these datasets. For some of them only a vague qualitative description can be found or, at most, some information about the surficial sediment is provided only for a near-by site. Therefore, in every case, we have attempted a good fit by choosing reasonable values for the input parameters. Table III lists the parameters: the Lambert constant μ_L (in dB); μ_v (in dB), and the resulting volume scattering cross-section m_o; as obtained by inverting Eq. (8). In all cases, for spectral calculations of rms roughness, partition wavenumber and slopes, the minimum wavelength allowed in the bottom roughness was set to $\lambda_a/1000$, where λ_a is the acoustic wavelength. The largest wavelength (footprint) was set to 128m.

For a power-law spectrum for the ocean floor described by Eq. (6), the roughness-related parameters needed in the model are calculated as follows:

(i) The mean squared microroughness (in m^2) is given by Eq. (4) with $g_\mu = 1$, i.e.,

$$\sigma_\mu^2 = 1 / 4\, k^2 \cos^2\theta \,. \qquad (17)$$

(ii) The partition spatial frequency (in cycles/m) is given by substituting σ_μ^2 from the above into Eq. (7), and solving the definite integral, i.e.,

$$K_c = [K_h^{\gamma} - \gamma / (8\pi a^2 \cos^2\theta)]^{(1/\gamma)} \,, \qquad (18)$$

where $\gamma = -2b+2$.

(iii) The mean-squared slope of the fine-scale surface is given by substituting K_c from the above into Eq. (8), i.e.,

$$\delta_{fo}^2 = [2\pi a^2/(\gamma+2)] \cdot [K_c^{(\gamma+2)} - K_l^{(\gamma+2)}] . \qquad (19)$$

Table III: Fitting parameters.

DATASET	f(kHz)	n	κ_p	μ_v(dB)	μ_L(dB)	m_o
byuk68_A2	2.8	0.975	0.15	-33.2	-25.0	9.8×10^{-5}
byuk68_A3	2.8	1.013	0.10	-33.7	-28.0	6.3×10^{-5}
hnby92_SA	0.9	0.919	0.04	-32.4	-30.0	9.3×10^{-6}
hnby92_SA	1.2	0.919	0.04	-37.1	-35.0	1.1×10^{-5}
hnby92_SA	2.3	0.919	0.04	-39.2	-37.0	4.9×10^{-6}
hnby92_SC	2.3	0.996	0.15	-29.0	-25.0	2.2×10^{-4}
jnel89	2.0	1.013	0.10	-47.0	-43.0	2.2×10^{-6}
mogy85	0.365	0.94	0.09	-33.1	-30.0	8.6×10^{-6}
scdt69_Stn3	3.2	1.001	0.10	-28.0	-27.0	3.0×10^{-4}
scdt69_Stn5	3.2	1.001	0.10	-34.0	-33.0	7.4×10^{-5}
vvzy74	5.0	1.013	0.10	-24.1	-23.0	1.0×10^{-3}
zvfn85	4.0	0.866	0.70	-35.2	-33.0	4.0×10^{-4}

Moderately Steep Incidence

We first present results corresponding to data at moderate grazing angles to normal incidence. Results for grazing incidence will be examined later. In all cases, along with the results of the present model, the prediction obtained by combining the rough facet model with Lambert's law is shown. Both the volume parameter μ_v and the Lambert constant μ_L are chosen to get their respective best fit. In Fig. 2 the fitting of dataset {jnel89}[21] is shown. This dataset corresponds to 2kHz in a slow sediment. Also shown in this figure are the relative contributions of the three components of Eq. (1) to the total scattering coefficient. There seem to be two well defined regimes: near normal incidence the result is controlled by the rough facet model (reflections at the rough facets) and at moderate to large incidence angles it is controlled by the volume component. The only significant contribution, if present at all, of resonant (Bragg) scattering at the microroughness scale occurs in the transition region (elbow of the curve). Figures 3a and 3b show results for dataset {scd69}[22] at 3.2kHz for two sites. In particular, in Fig. 3b, the model mimics well the transition between the specular lobe and the middle angular range plateau, indicating that the three components to the scattering coefficient are adequately combined. Figure 4 corresponds to dataset {vvzy74}[23] at 5 kHz. The model handles the transition region quite well. It should be noted that, for these examples involving moderate steep angles, plays a crucial role.

Shallow Grazing Incidence

Let us now examine the case of shallow grazing angles. Figure 5a shows results for dataset {hnby92_SA}[4] at 900 Hz. This dataset corresponds to a site in the Sohm Abyssal Plain which has a fast sandy bottom. The data displays a hump near grazing which, according to the modeling, occurs in the vicinity of the critical angle. Since attenuation is being taking into account, total reflection does not occur. Lambert's law is blind to this anomaly. Figures 5b and 5c show results at 1.2 and 2.3kHz for the same site. In the three cases the proposed model tracks the data fairly well. Figure 5d shows results for site C at 2.3kHz. In this case there is no hump and the model departs from data at shallow grazing angles. To "erase" the hump from the model, an attenuation factor higher than the one used for site A was adopted. This choice, when combined with the best choice for μ_v, in turn leads to a higher volume scattering cross section than in previous examples. In this particular dataset, Lambert's law (also shown in Fig. 5d) does a better job than the current model. Figures 6a and 6b show results for datasets {byuk68_A2}[24] and {byuk68_A3}[24], respectively, corresponding to two different sites with the same frequency (2.8kHz). In the first case the bottom was modeled as a fast bottom to get the hump at the critical angle. For the second case a slow bottom was assumed (see Table II). In both cases the fitting is satisfactory. Lambert's law cannot track the data. Figure 7 shows the fitting for dataset {zvfn85}[25] at 4kHz and Fig. 8 for dataset {mogy85}[26] at 365Hz. In both cases the model does an excellent job in tracking the data, while Lambert's law fails to mimic the shallow angles.

Discussion

The role of the different environmental parameters in fitting data varies with the angular region. Near normal incidence the spectral parameters a and b control the lobe through δ_f and σ_μ. The impedance mismatch plays a minor role and the volume contribution is negligible. At large incidence angles the fitting strongly depends on the volume scattering cross-section m_o and, to a lesser degree, on both the rms slope of the large surface (it controls the rate of decay near grazing) and the impedance contrast. For fast sediments, where a critical angle exists, the attenuation factor κ_p controls the amplitude of the hump. In the case of slow sediments the effect of κ_p is negligible for fitting purposes. It plays a role only when backing out m_o from μ_v through Eq. (9). Figures 9 and 10 show the sensitivity of the fitting to changes in theattenuation coefficient κ_p and in the rms slope of the fine-scale surface (δ_f) for large incidence angles (near grazing incidence).

The backscattering-derived volume scattering coefficient (m_o) is extracted from the fitting constant μ_v. Although the magnitude of the volume scattering coefficient (m_o) can change by almost an order of magnitude just by changing κ_p for slow sediments, the fitting for μ_v is almost insensitive to κ_p. On the other hand for fast

sediments, the fitting is more sensitive to κ_p and, therefore, the value of m_o is more robust. The resulting values for m_o are within the order of magnitude of those reported in the literature, obtained also, in all cases, through indirect methods. However, due to the crude averaging process adopted for the volume contribution, the value of m_o should be considered a rough estimate of the true value. Future work will be oriented to relate the free parameter μ_v (and therefore m_o) with the type of surficial sediment.

IV. CONCLUDING REMARKS

A simple model for estimating the bottom backscattering strength for low to moderately high frequencies has been set forth. This model combines a Helmholtz/Kirchhoff two-scale scattering model with Ivakin and Lysanov's volume scattering model, and with resonant scattering from the microroughness. The model does not assume any specific scattering mechanism within the sediment, and aims toward a rapid but reliable estimation of the scattering strength from a gross classification of the type of surficial sediment and physiographic region (abyssal plain, continental rise, shelf, etc). It contains only one free parameter proportional to the volume scattering cross-section per unit volume. The model performs reasonably well under a variety of conditions. The surface roughness seems to control mainly the angular region near normal incidence (specular lobe), and the volume scattering dominates at moderate to large angles of incidence. The resonant contribution from the microroughness dominates the transition angular range between the two regions. It will also control the shallow-grazing incidence in cases where the impedance missmatch prevents penetration and the volume contribution is weak. The attenuation in the sediment seems to play a role in scattering for fast sediments. For slow sediments, on the other hand, the model is basically insensitive to variations in the attenuation.

V. ACKNOWLEDGEMENTS

This work was funded by the Naval Research Laboratory High-Frequency Basic Research Program and the Office of Naval Research Acoustic Reverberation Special Research Program.

REFERENCES

1. P.A. Crowther, "Some statistics of the sea-bed and scattering therefrom," in Acoustics and the Sea-Bed, 147-156, ed. N. G. Page, Bath Univ. Press., Bath (1983).

2. D.R. Jackson, D.P. Winebrenner, and A. Ishimaru, "Application of the composite roughness model to high frequency bottom backscattering," J. Acoust. Soc. Am., **79**, 1410-1422 (1986).

3. P.D. Mourad and D.R. Jackson, "A model/comparison for low frequency bottom backscatter," J. Acoust. Soc. Am., **94**, 344-358 (1993).

4. P.C. Hines and P.J. Barry, "Measurements of acoustic backscatter from Sohm Abyssal Plain," J. Acoust. Soc. Am., **92**, 315-323 (1992).

5. C. de Moustier and D. Alexandrou," Angular dependence of 12-kHz seafloor acoustic backscatter," J. Acoust. Soc. Am., **90**, 522-531 (1990).

6. H. Matsumoto, R.P. Dziak, and C.G. Fox, "Estimation of seafloor microtopographic roughness through modeling of acoustic backscatter data recorded by multibeam sonar systems," J. Acoust. Soc. Am., **94**, 2776-2787 (1993).

7. J.H. Stockhausen, "Scattering from the volume of an inhomogeneous half-space," Naval Research Establishment, Canada, Report No. 63/9.

8. Yu.Yu. Zhitkovskii, "Sound scattering by inohmogeneitioes of the ocean bottom," Izv. Atmoss. and Ocean Phys., 567-571 (1968).

9. A.N. Ivakin and Yu.P. Lysanov," Underwater sound scattering by volume inhomogeneities of a bottom medium bounded by a rough surface," Sov. Phys. Acoust., **27**, 212-215 (1981).

10. A. Lyon and A.L. Anderson, "Acoustic scattering fro the sea floor: Modeling and data comparison," J. Acoust. Soc. Am., **95**, 2441-2451 (1994).

11. K.V. Mackenzie, "Bottom reverberation for 530 and 1030 cps sound in deep water," J. Acoust. Soc. Am., **33**, 1498-1504 (1961).

12. W. Geddes, Personnal Communication (1994).

13. D.D. Ellis and D.R. Haller," A scattering function for bi-static reverberation calculations," J. Acoust. Soc. Am., **82**, S124 (1987).

14. J.W. Caruthers and J.C. Novarini, "Modeling Bistatic Bottom Scattering strength including a forward lobe," IEEE J. Oceanic Engr., **18**, 100-107 (1993).

15. L.M. Brekovskikh and Yu.P. Lysanov, Fundamentals of Ocean Acoustics, Springer Verlag, Berlin (1982).

16. J.C. Novarini and J.W. Caruthers, "The partition wavenumber in acoustic backscattering from a two-scale surface described by a power-law spectrum," IEEE J. Oceanic Engr., **19**, 200-207 (1994).

17. E.L. Hamilton, "Geoacoustic modeling of the seafloor," J. Acoust. Soc. Am., **68**, 1313-1340 (1980).

18. The "Lommel/Zeeliger" law is often cited in the literature of the Former Soviet Union, e.g., Ref. 9, but we have not found the original reference to this form.

19. A.N. Ivakin and Yu.P. Lysanov, "Backscattering of sound from an inhomogeneous bottom at small grazing Angles," Sov. Phys. Acoust., **31**, 236-237 (1985).

20. L. Zhang, "SBBS-LD: A database for sea bottom backscattering measurement data.: Low frequency, deep ocean," Tech Rep. Center for Marine Science, Univ. of Southern Mississippi (1992).

21. G. Jin, " Deep water reverberation measurements in the South China Sea," Technical Acoustics, **8**, 8-11 (1989).

22. P.B. Schmidt, " Bottom reverberation in the Norwegian Sea and North Atlantic Ocean," Informal Report, U.S. Naval Oceanographic Office, IR#69-38 (1968).

23. V.I. Volovov and Yu.Yu. Zhitkovskii, " Reflection and scattering of sound by the ocean bottom," Acoustic of the Ocean Part 6, Ed. L. M. Brekovskikh Joint Publication Research Series, Arlington Virginia 197-234 (1975).

24. J.P. Buckley and R.J. Urick, "Backscattering from deep sea bed at small grazing angles," J. Acoust. Soc. Am., **44**, 648-650 (1968).

25. A.I. Zotov and A. V. Folkin, "On investigating the local characteristics of sound scattering by deep ocean sediments," Oceanology, **25**, 165-168 (1985).

26. D. Maradino and T. G. Goldsberry, "Evaluationof low frequency backscattering strength vs grazing angle by mean of multiple beamforming," in Ocean Seismo-Acoustics: Low frequency Underwater Acoustics, Ed. T.Akal and J. Berkson, Plenum Press, N.Y., 355-364, 1985

[This page is left blank intentionally]

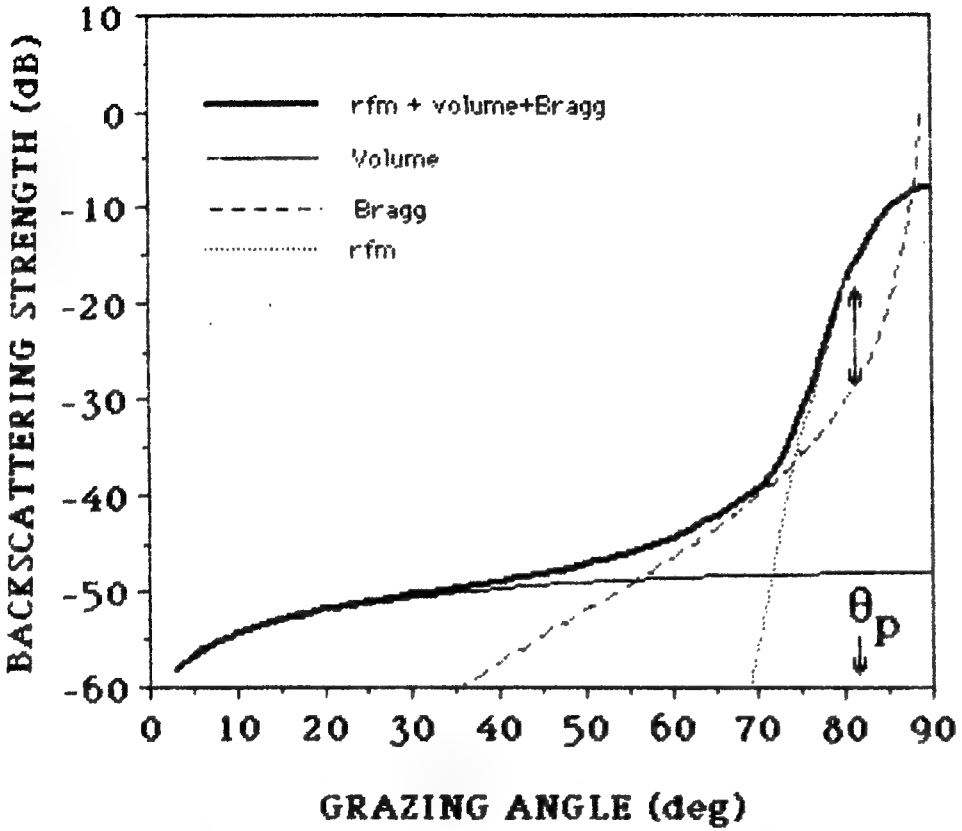

Figure 1: Disclosure of the contributions of each term of Eq.(1) to the total backscattering stength. θ_p denotes the crossover angle at which resonant scattering at the microroughness starts to contribute. The scattering coefficients, m_μ, m_f, and m_v are labelled by their respective models, Bragg, RFM, and volume. The overall scattering coefficient, m_{bs}, is given by the solid curve.

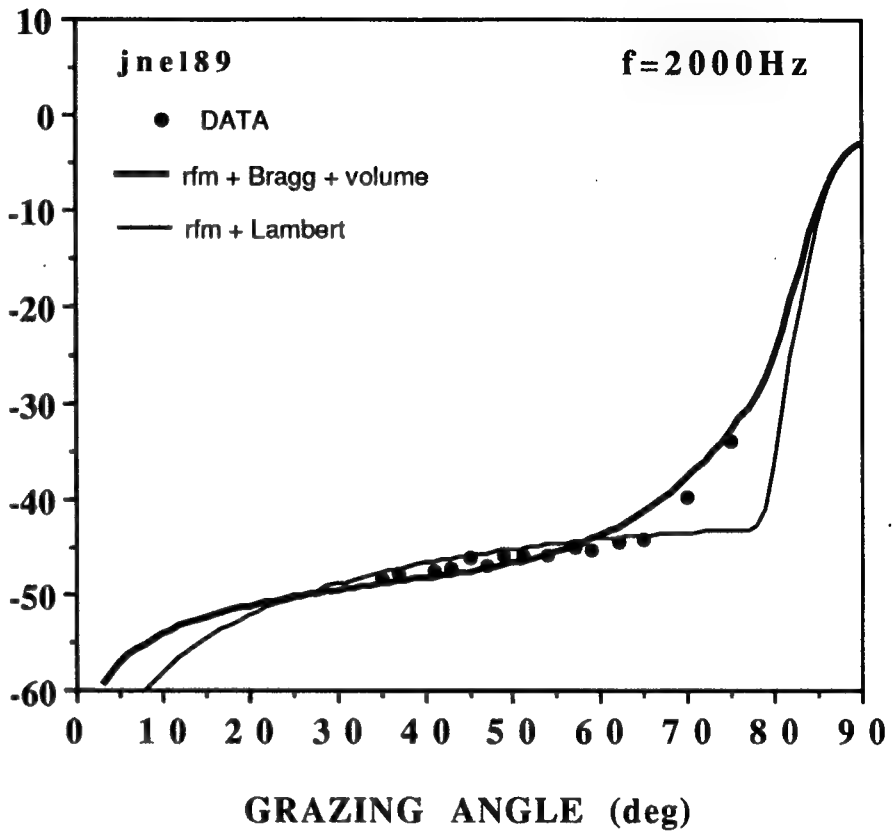

Figure 2: Data fitting for a deep water site in the South China Sea.[21]

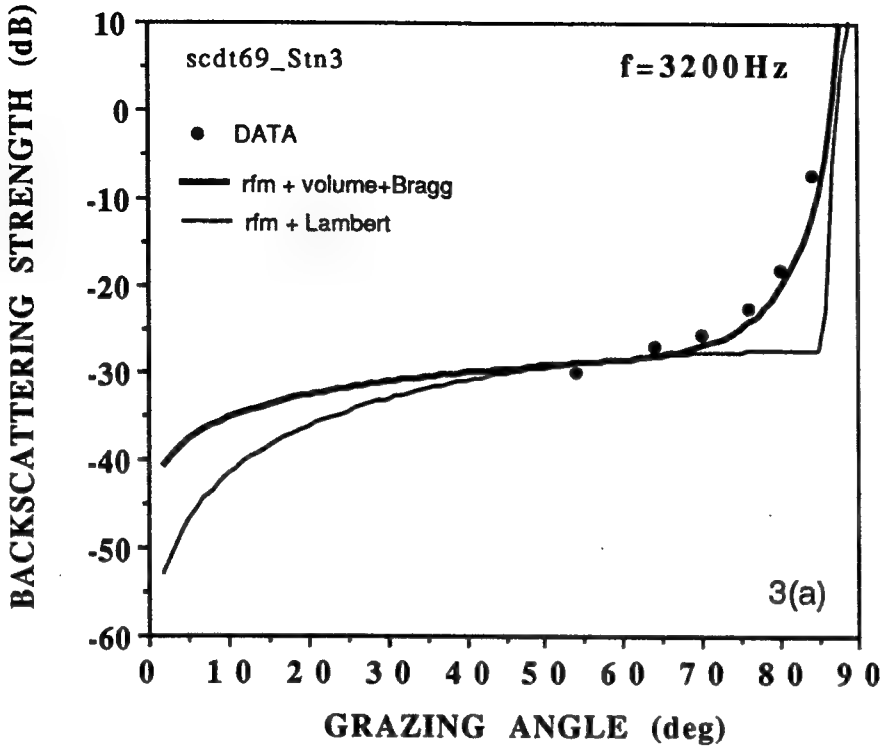

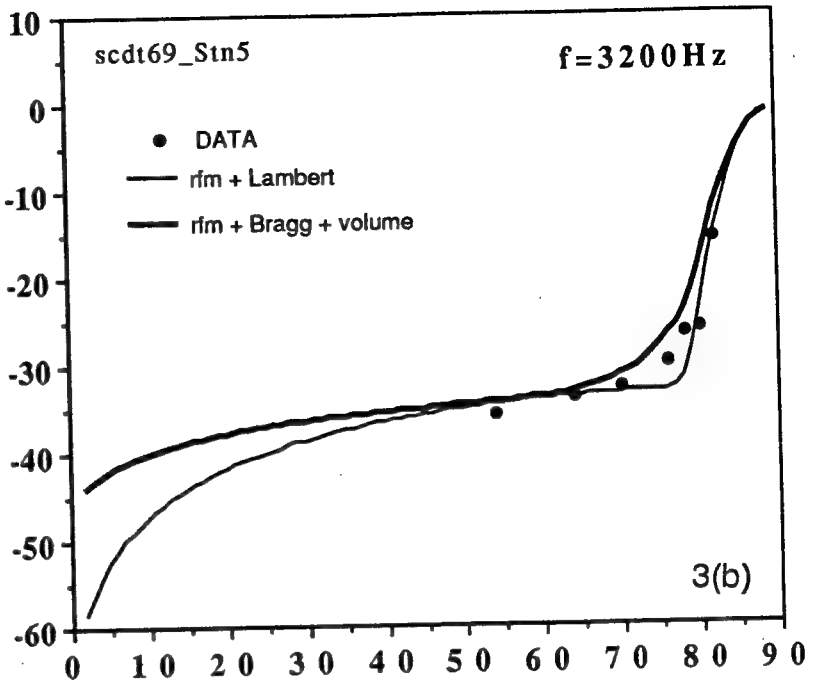

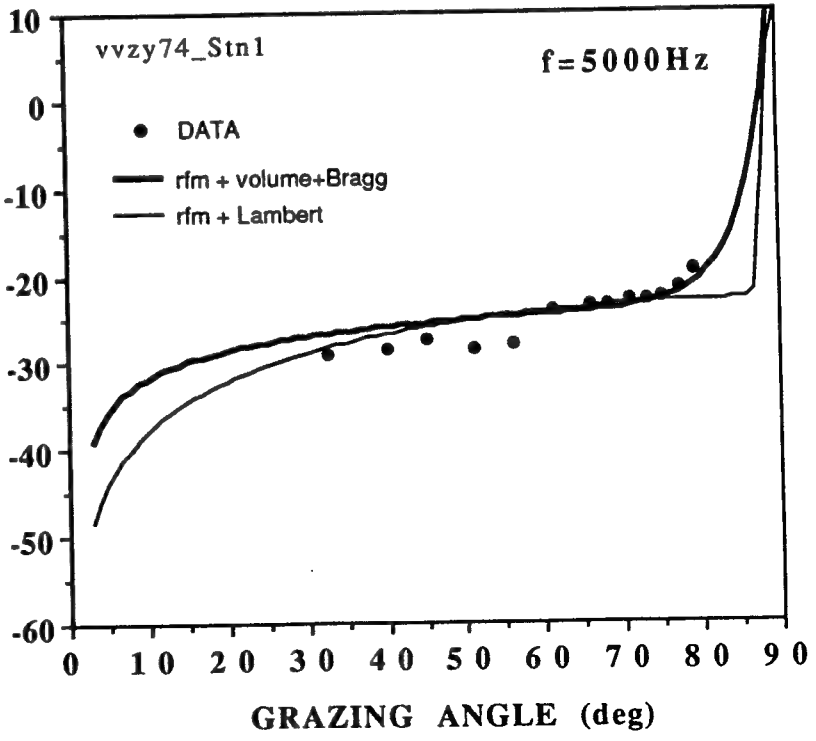

Figure 3: Comparison of backscattering model and data for the North Atlantic Continental Slope, (a) Station 3 and (b) Station 5.[22]

Figure 4: Comparison of backscattering model and data from Volovov and Zhitkovskiy corresponding to a site in the North Atlantic.[23]

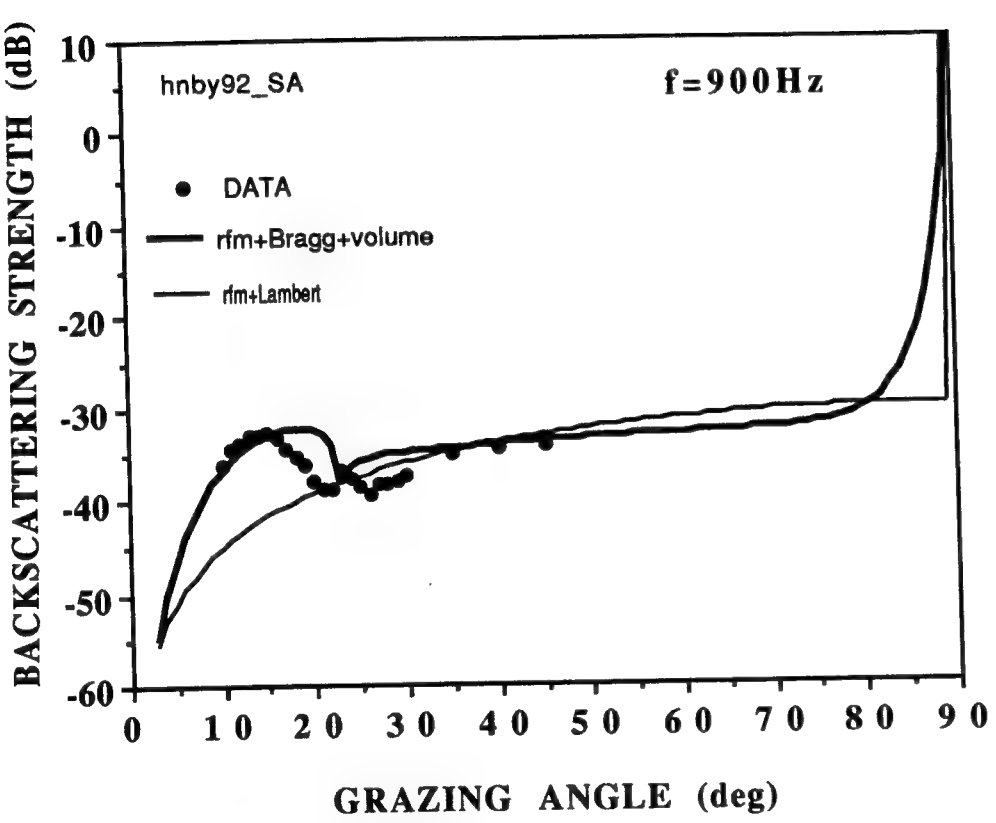

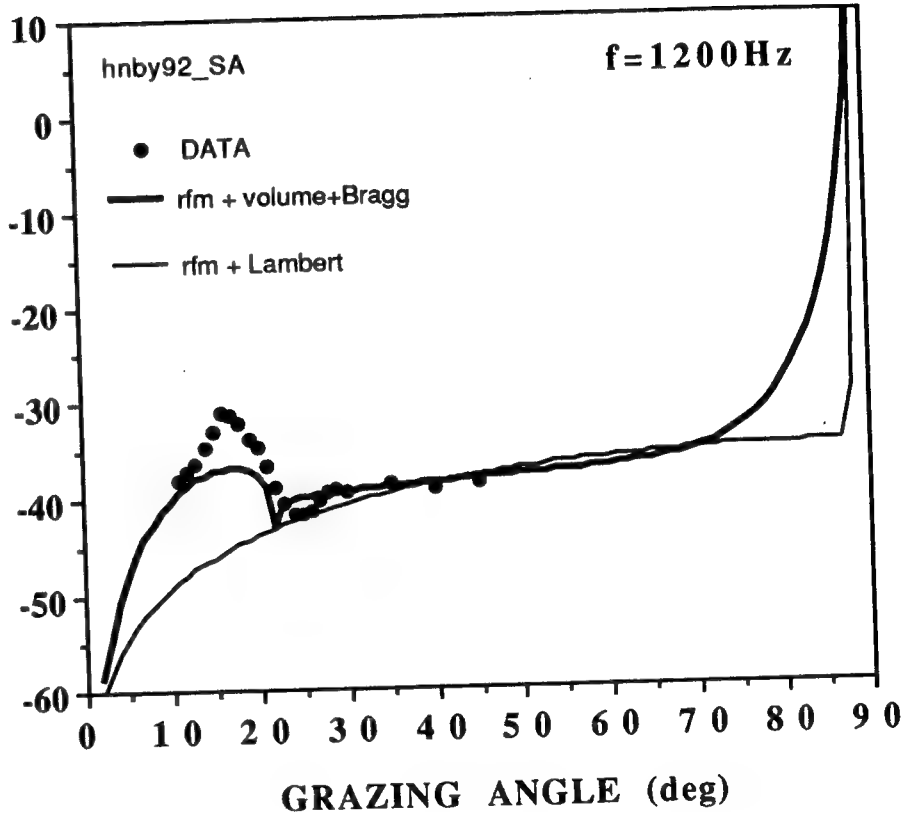

Figure 5(a,b): Comparison of backscattering model and data from Hines and Barry corresponding to the Sohm Abyssal Plane (a) Site A, f=900Hz and (b) Site A f=1200Hz.[4]

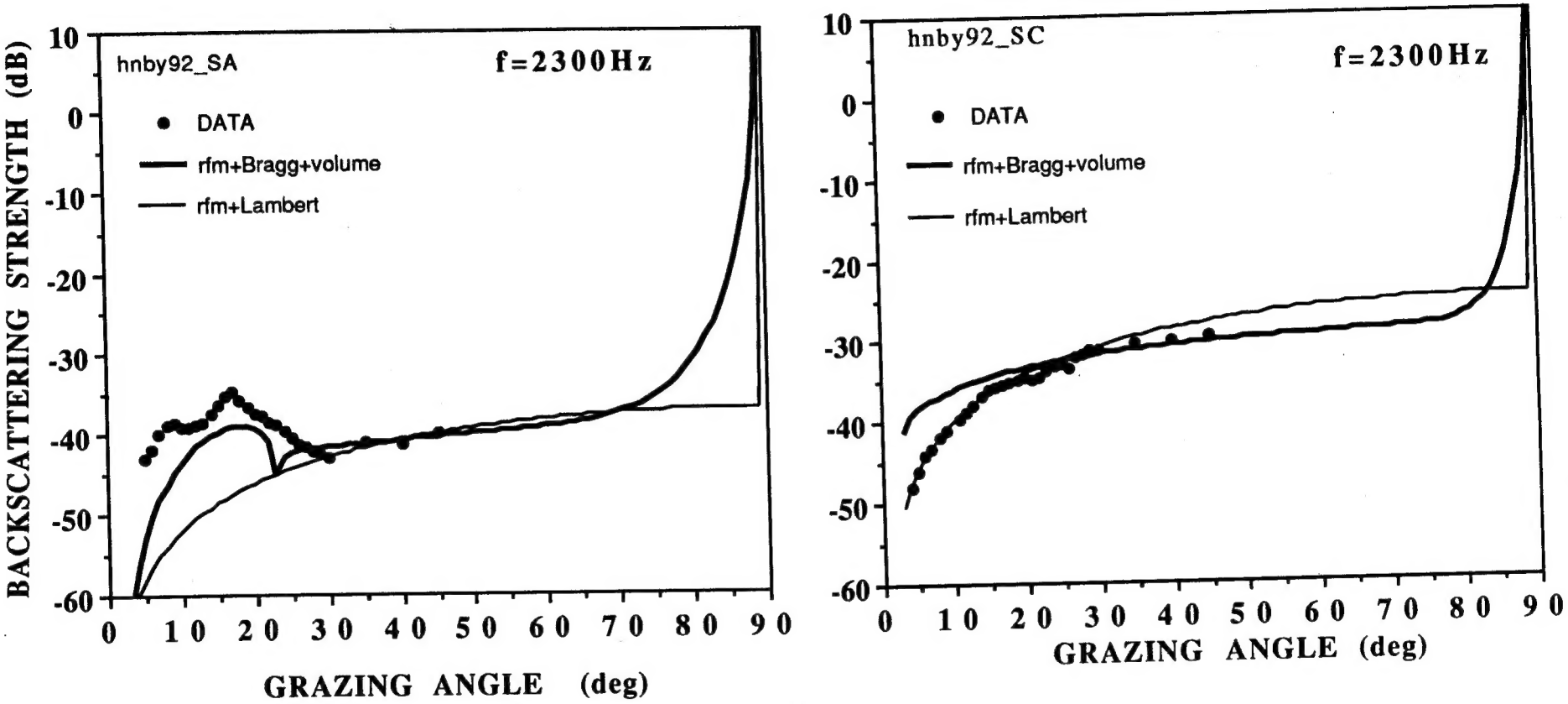

Figure 5(c,d): Comparison of backscattering model and data from Hines and Barry corresponding to the Sohm Abyssal Plane (c) Site A f=2300Hz; and (d) Site C f=2300Hz.[4]

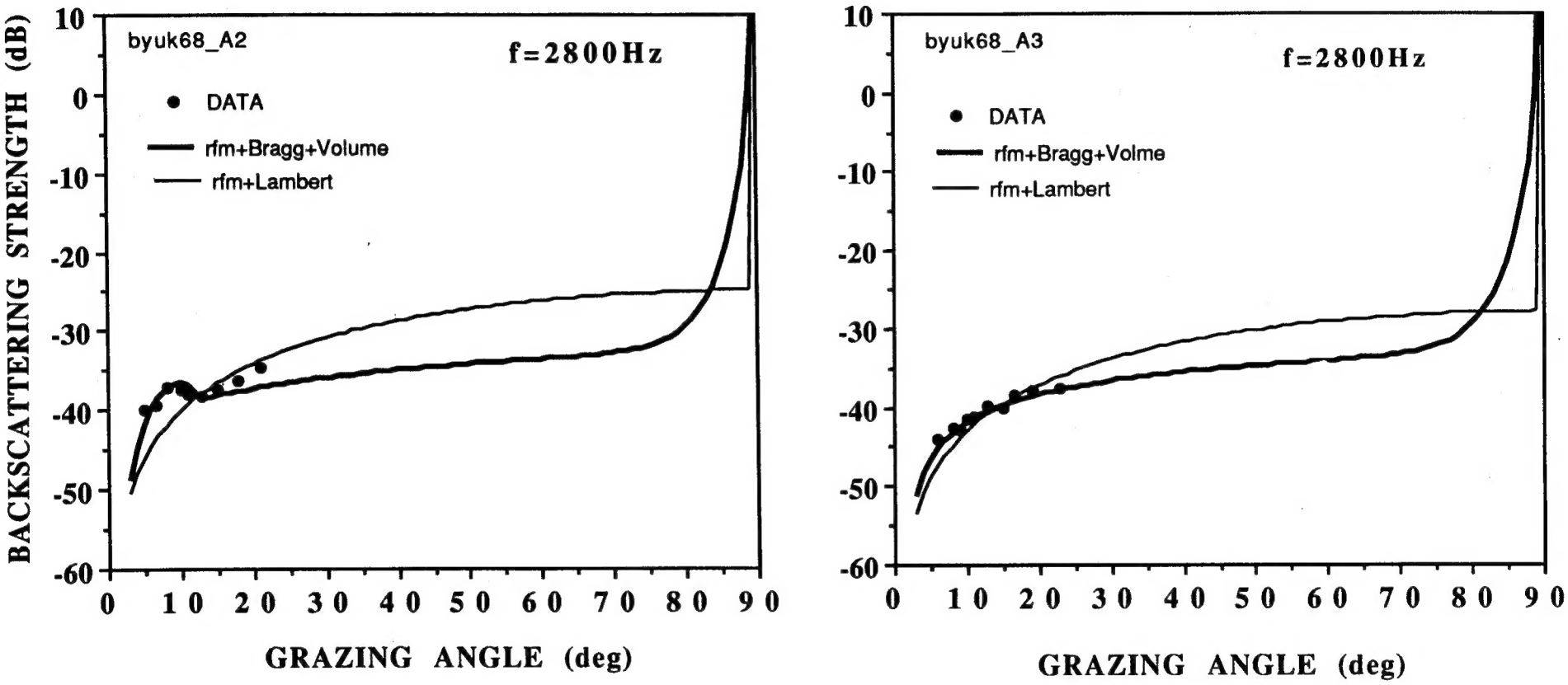

Figure 6: Comparison of backscattering model and data from Buckley and Urick corresponding to the North American Continental Rise (a) Area II, (b) Area III.[24]

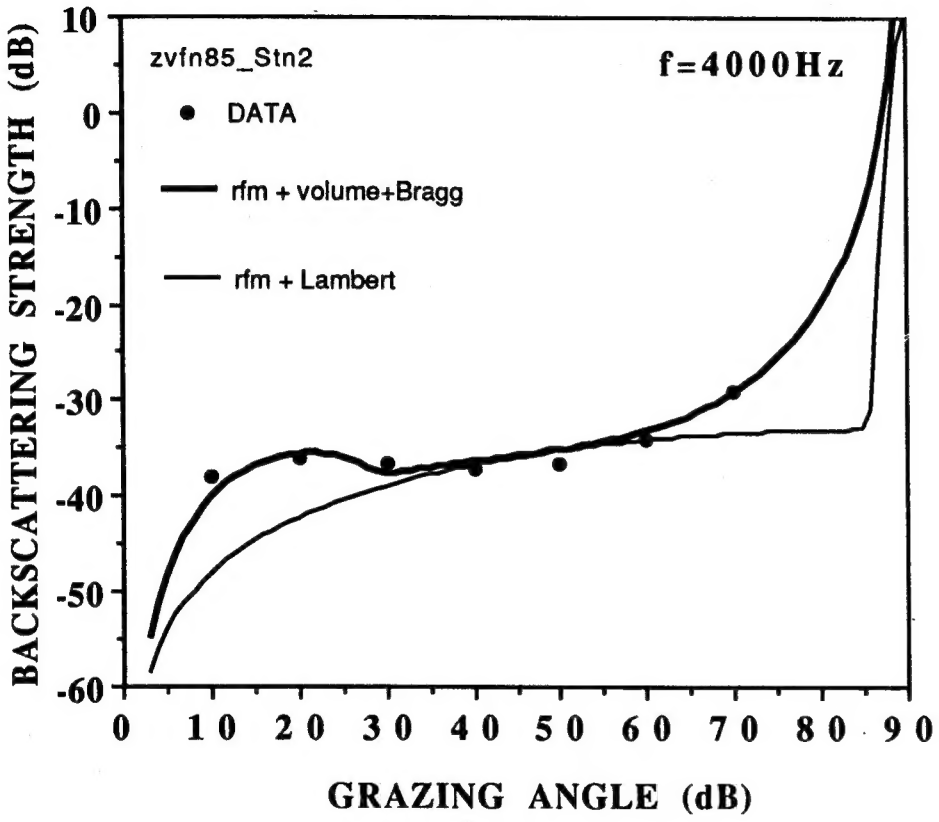

Figure 7: Comparison of backscattering model and data from Zotov and Fokin on a site on the Clipperton Fault.[25]

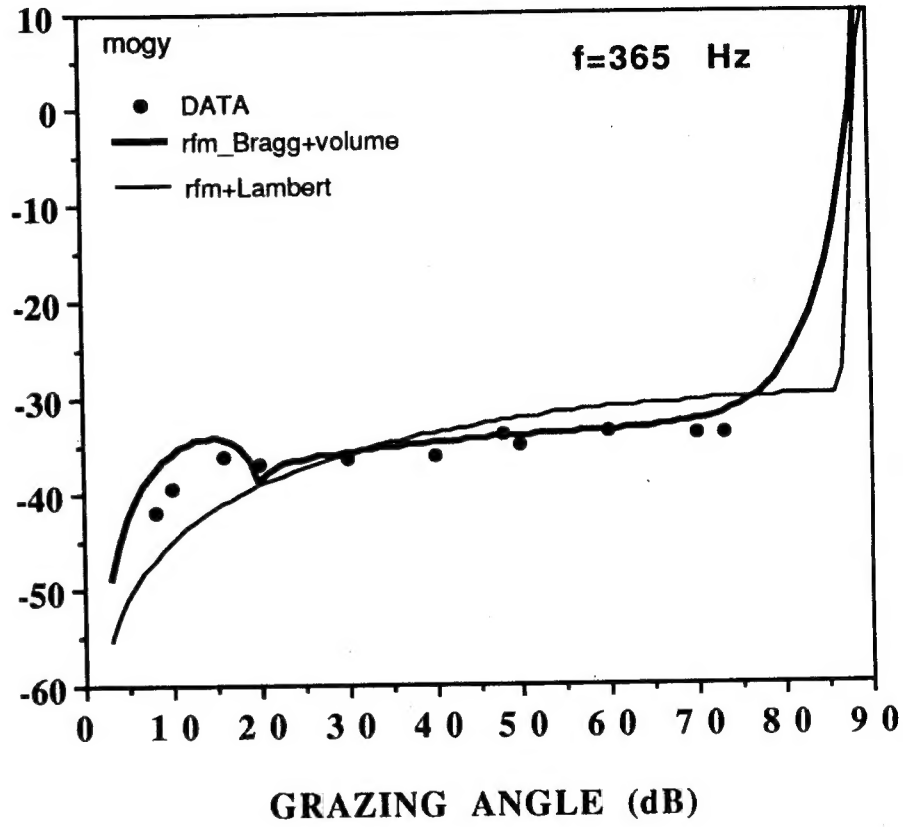

Figure 8: Comparison of backscattering model and data from Maradino and Goldsberry in the North Atlantic Abyssal Plain.[26]

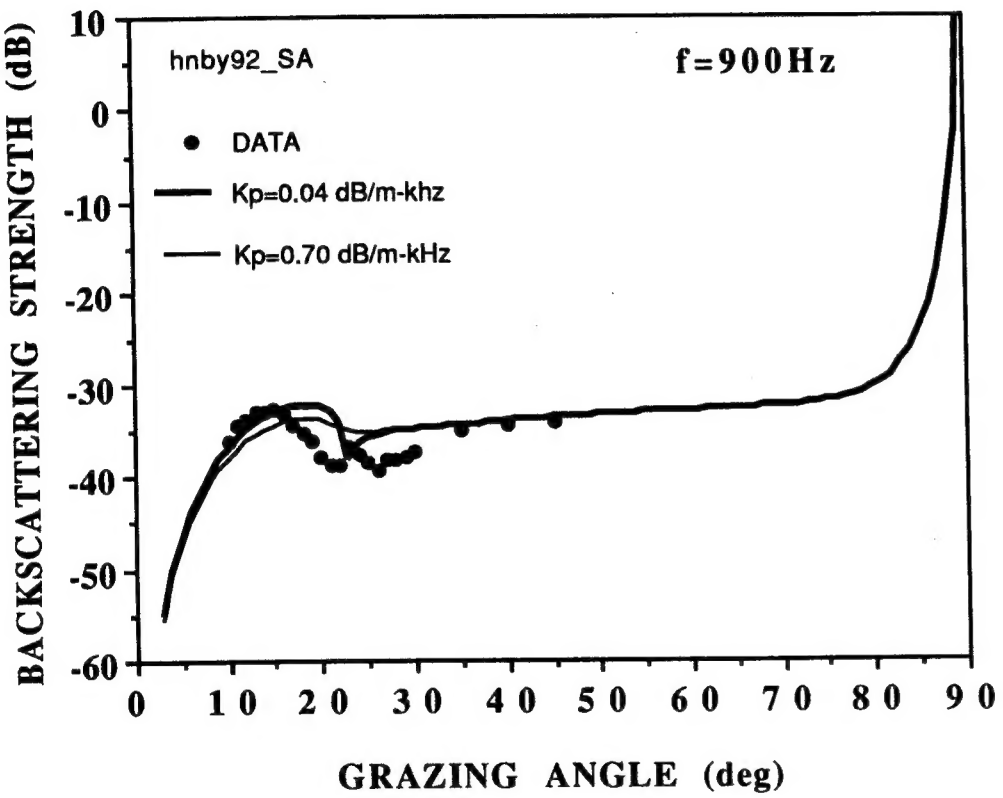

Figure 9: Sensitivity of the fitting to changes in the attenuation factor κ_p, and on the rms slope of the large scale surface for the case of a fast sediment.[4]

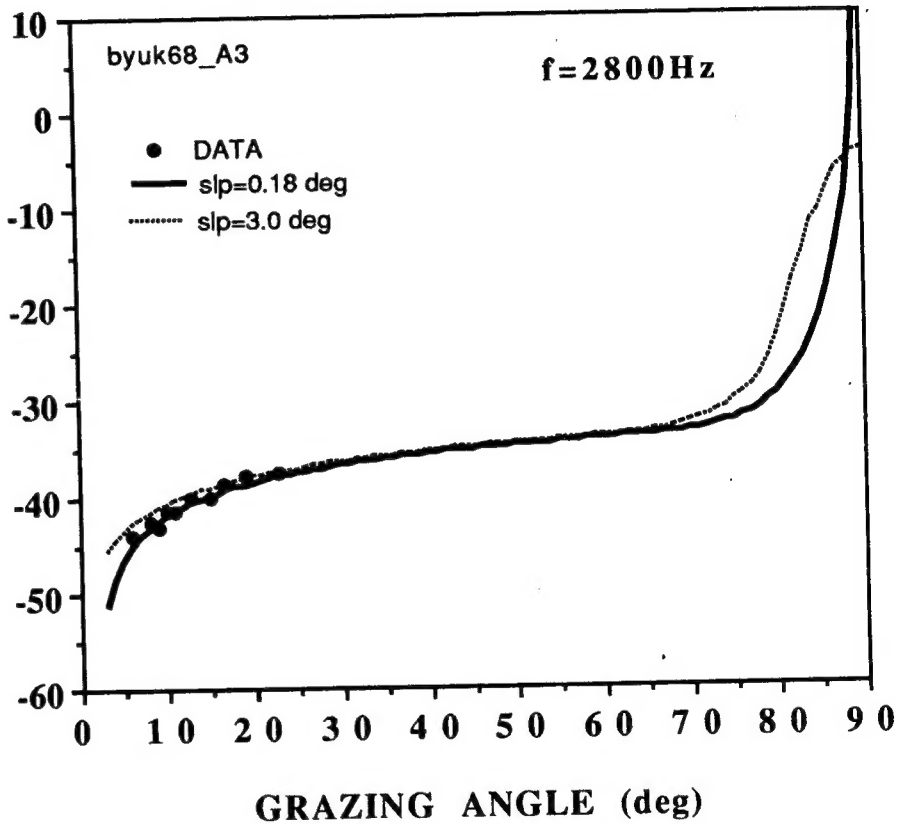

Figure 10: Sensitivity of the fitting to changes in the attenuation factor κ_p, and on the rms slope of the large scale surface.[24]